

High-Gain, Polarization-Preserving, Yb-Doped Fiber Amplifier for Low-Duty-Cycle Pulse Amplification

Introduction

Erbium-doped fiber amplifiers have become commonplace in telecommunications systems.¹ High-bit-rate pulse trains mean that continuous pumping can be utilized. Additionally, the unknown polarization state of the arriving pulses is ideal for common fiber-optic components and erbium-doped fibers, which typically do not preserve the polarization state of the light passing through them. For other applications, however, such conditions do not apply. Low-duty-cycle pulses leave gain available in the fiber for long durations between pulses, which can lead to parasitic lasing or destructive self-pulsations. The amplification of signals with wavelengths far from the gain peak only enhances this problem since the gain can be substantially lower for such signals. Additionally, the amplification of linear polarizations requires not only a polarization-maintaining (PM) active fiber, but also PM wavelength division multiplexers (WDM's) and other fiber components that can be difficult to fabricate.

Utilizing a double-pass configuration allows for significantly higher gains to be obtained in a single-fiber amplifier than can be achieved in a single pass.²⁻⁵ Additionally, using a Faraday rotator just before the end mirror ensures that the pulse returning from the second pass through the cavity has a polarization state that is orthogonal to that of the input pulse. Consequently, when used in conjunction with a polarizing beam splitter, the output pulse can be separated from the input pulse with high fidelity.³ Double-pass configurations are ripe for parasitic lasing or destructive self-pulsations in a highly pumped unsaturated amplifier, however, since half a resonator is created intentionally. Special care must be taken to minimize reflections from components, connectors, and splices. Utilizing a timed gate, e.g., an acousto-optic modulator (AOM), at the end of the first pass can ensure stable operation,³ but this significantly adds to the complexity of the system.

In this work, a double-pass, ytterbium-doped fiber amplifier is presented that overcomes these hurdles to provide high gain for low-duty-cycle pulse repetition rates while preserving the linear polarization state in a single-spatial-mode package that

requires no alignment. In **Amplified Spontaneous Emission Considerations** (p. 63) the amplified spontaneous emission (ASE) is modeled in ytterbium-doped fiber amplifiers. In particular, the effects of ASE filtering are studied for use in a double-pass amplifier configuration. The **Experimental Results** (p. 66) are presented on the measurements of a double-pass fiber amplifier built with the various ASE-suppression schemes described in **Amplified Spontaneous Emission Considerations**. Additional discussions regarding the experimental configuration and modeling are given in **Discussion and Conclusions** (p. 68), along with concluding remarks.

Amplified Spontaneous Emission Considerations

The amplified spontaneous emission of fiber amplifiers can be studied via rate-equation modeling.⁶ Such a model represents the optical power resolved in wavelength along the length of the fiber and the ytterbium atomic states as a homogeneously broadened inversion. The resultant equations are given by

$$\pm \frac{\partial P^\pm}{\partial z} + \frac{1}{v_g} \frac{\partial P^\pm}{\partial t} = \Gamma[\sigma_e N_2 - \sigma_a N_1]P^\pm - \alpha P^\pm + 2\sigma_e N_2 \frac{hc}{\lambda^3} \Delta\lambda + S\alpha_{RS}P^\mp \quad (1)$$

and

$$\frac{\partial N_2}{\partial t} = \frac{1}{hc} \int \frac{\Gamma}{A} [\sigma_e N_2 - \sigma_a N_1] (P^+ + P^-) d\lambda - \frac{N_2}{\tau}, \quad (2)$$

where $P^\pm(z, t, \lambda)$ is the forward (+) or backward (-) propagating power as a function of wavelength, time, and axial position along the fiber. N_2 and N_1 are the upper and lower state population densities, respectively, as a function of time and axial position along the fiber and are related by the total ion concentration as $N_t = N_2 + N_1$, which is constant throughout the fiber. Wavelength-dependent parameters in Eqs. (1) and (2) include the geometrical overlap of the fiber mode with the core Γ , modal area A , absorption/emission cross section of the active ion $\sigma_{a/e}$, group velocity v_g , fiber attenuation α , and Rayleigh scattering coefficient α_{RS} . Additional parameters include the upper-state lifetime τ , the fiber-core capture coefficient S , and the optical sampling bandwidth $\Delta\lambda$.

Equation (1) represents the bidirectional power flow through the fiber, including stimulated emission, spontaneous emission, and absorption from the active ions; loss due to the inherent fiber attenuation; and Rayleigh scattering. Since the parameters all have wavelength dependence, only a single equation is mathematically required to represent the behavior of the pump, signal, and ASE.

Equation (2) represents the excited-state population density, which is governed by the absorption and emission of optical power as well as nonradiative decay. One notable omission in Eq. (2) is the wavelength dependence of the excited state governed by the details of the atomic transition manifold. This leads to, for example, excitation due to the absorption of long-wavelength light that can then be used to amplify shorter wavelength light. While this effect is small in the presence of a highly inverted fiber, the impact on the current work is to overestimate the ASE at the gain peak. Since the current goal is to suppress this feature, the model will yield a worse case than is expected experimentally.

For simplicity, the wavelength dependence of A , v_g , α , and α_{RS} are neglected. Since the current work considers core-pumped (as opposed to cladding-pumped) active fibers, Γ can also be well approximated by a constant. The ytterbium cross sections are obtained from the data in Ref. 7. For convenience, these cross sections are fit to a series of Gaussians of the form

$$\sigma_j = \sum_m A_{j,m} \exp\left\{-\left[\frac{\lambda - \lambda_{j,m}}{w_{j,m}}\right]^2\right\}$$

with the coefficients listed in Table 106.I. Other utilized parameters are listed in Table 106.II.

Table 106.I: Gaussian coefficients for ytterbium emission and absorption cross sections.

j	$A_{j,m}$ (10^{-27} m ²)	$\lambda_{j,m}$ (nm)	$w_{j,m}$ (nm)
a	180	950	70
a	360	895	24
a	510	918	22
a	160	971	12
a,e	2325	975	4
e	160	978	12
e	340	1025	20
e	175	1050	60
e	150	1030	90

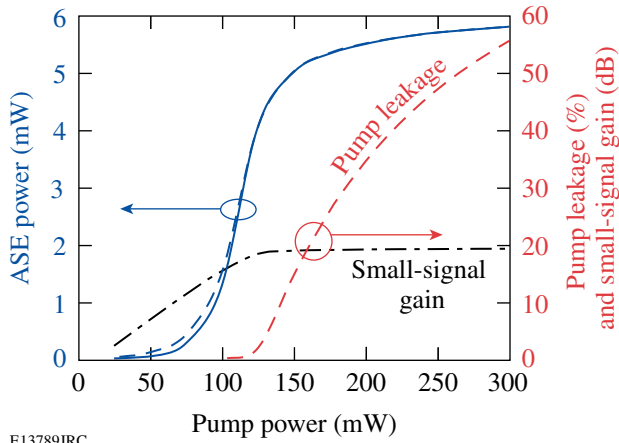
Table 106.II: Parameters used in simulations.

Parameter	Value
N_t	9.4×10^{24} m ⁻³
Γ	0.85
A	$30 \mu\text{m}^2$
v_g	$c/1.5$
α	0.003 m ⁻¹
$S\alpha_{RS}$	1.2×10^{-7} m ⁻¹
τ	0.84 ms
$\Delta\lambda$	1 nm
λ_{pump}	976 nm
λ_{signal}	1053 nm

Data provided with the ytterbium-doped fiber (Nufern), along with our own measurements on the fiber, determined the values of N_t , Γ , and A . The other values were obtained from Ref. 6. The parameters used are compiled in Table 106.II. A simple finite-difference method is utilized to calculate the power and inversion distributions in the fiber. Initial conditions assume no optical power or inversion within the fiber, and the pump power is included as a boundary condition. A double-pass configuration can also be realized by applying the appropriate boundary conditions.

Unsaturated fiber amplifiers cannot be pumped to arbitrarily high levels because of self-pulsations and oscillation, which limit the length of fiber that can be practically used in a single-pass amplifier. In an unsaturated amplifier this translates to limited available gain. Figure 106.1 shows the forward and reverse amplified spontaneous emission for the case of reverse pumping and very weak signal amplification (no gain depletion) for a 3.5-m length of Yb: fiber with the characteristics in Table 106.II. The small-signal gain, defined as the ratio of output energy to input energy, for a 1053-nm signal and the pump leakage are also shown in this figure. After 140 mW of pump power, the fiber is almost completely inverted, and the remaining pump is lost out of the opposite end of the fiber. The small-signal gain 23 nm off the gain peak is therefore limited to approximately 20 dB.

Since the gain is in fact unsaturated, simply sending the signal back through for a second pass increases the amplification without additional pumping. Such a double-pass configuration, however, also allows the ASE to make a second trip through the gain, which can lead to undesirable oscillation



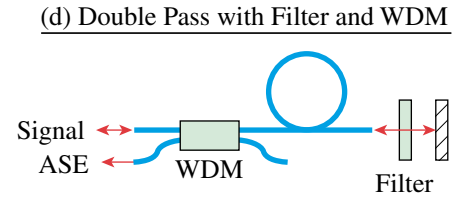
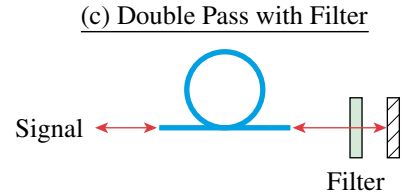
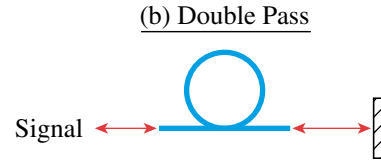
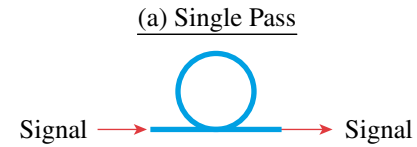
E13789JRC

Figure 106.1

Total (spectrally integrated) forward (solid) and reverse (dashed) ASE, 976-nm pump leakage, and 1053-nm small-signal gain as a function of pump power for a 3.5-m-length Yb: fiber.

and self-pulsations. The ASE must therefore be filtered to use a double-pass configuration. Two simple methods of filtration were investigated, as depicted in Fig. 106.2. The first is a bandpass filter, which is inserted between subsequent trips through the active fiber to deny double-pass ASE except in a small bandwidth around the filter peak. The second is a WDM designed to split the ASE peak from the signal, which removes a significant fraction of the ASE power from the signal, provided the signal is not near the gain peak. Four different amplifier configurations are modeled, as shown in Fig. 106.2. The first two are simple single- and double-pass configurations through the fiber. In the third configuration, a bandpass filter is added between subsequent passes through the fiber. The fourth configuration adds a WDM filter to the output of the third configuration.

For these calculations, the filters are assumed to be lossless at the transmission peaks with zero transmission at the nulls. The mirror adds 1 dB of loss to the double-pass amplifiers. Assuming pump and signal wavelengths of 976 and 1053 nm, respectively, the total (spectrally integrated) ASE power out of the different amplifier configurations is shown in Fig. 106.3 as a function of pump power. Because of undepleted gain and pump leakage, the single-pass ASE has a maximum power below 6 mW. In the double-pass configuration, the amplifier becomes saturated by the ASE, which extracts a significant fraction of the gain in the fiber. This linear trend in the ASE growth with pump power leads to an ASE level that is greater than 25 times the single-pass case and means that there will be very limited reduced gain available for the signal. In contrast, the dotted trace shows that the insertion of the bandpass filter



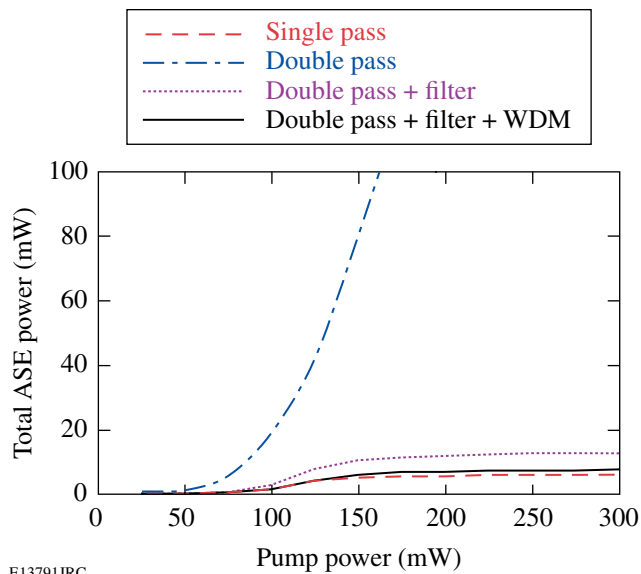
E13813JRC

Figure 106.2

Depiction of modeled configurations for (a) single pass, (b) double pass, (c) double pass with an intracavity bandpass filter, and (d) the same as (c) with a WDM filter at the amplifier output.

prohibits the ASE closest to the gain peak from experiencing double-pass gain. The total ASE is therefore limited to small-signal amplification, even with double-pass amplification far off the gain peak, and accumulates no more than twice the power of the single-pass configuration. The insertion of this filter then allows for exponential signal gain from the double-pass amplifier. The addition of the WDM filter (solid curve) reduces the total ASE output power of the double-pass fiber amplifier to only 30% more than the single-pass ASE.

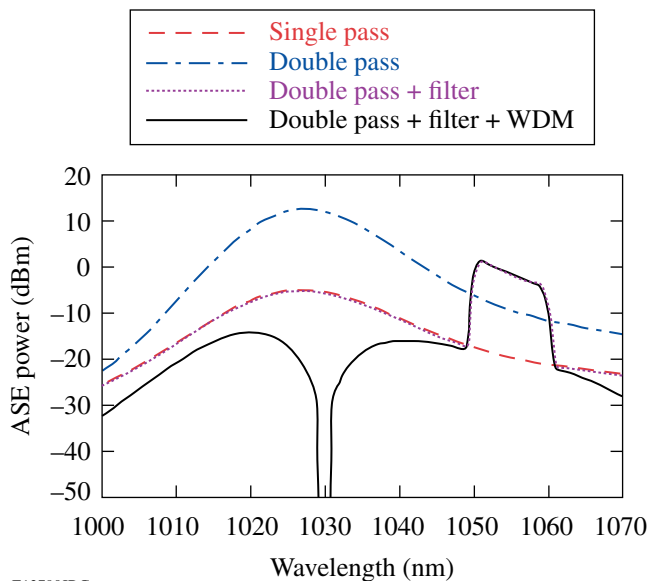
The ASE spectra for the four configurations are shown in Fig. 106.4 at a pump power of 250 mW. The ASE within the bandpass filter is actually stronger than the unfiltered double-pass ASE since the gain is unsaturated. Nonetheless, this lack of gain saturation allows for double-pass gain of the signal in the amplifier. The bandpass filter is therefore critical for operation of this double-pass configuration for the amplification of signals off the gain peak.



E13791JRC

Figure 106.3

Total (spectrally integrated) ASE power at the amplifier output as a function of pump power for the configurations shown in Fig. 106.2 using the fiber from Fig. 106.1.



E13790JRC

Figure 106.4

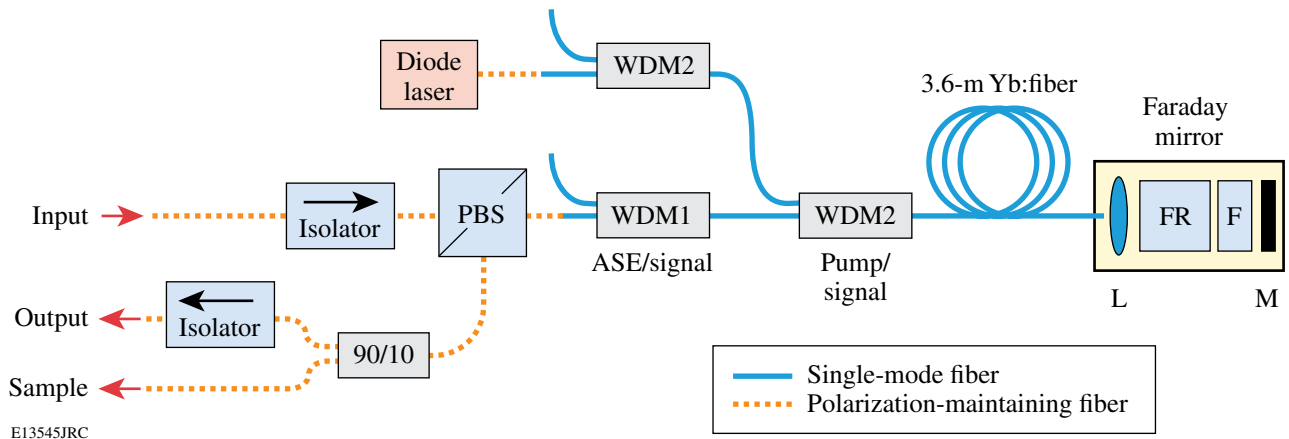
Amplified spontaneous emission spectra at the amplifier output for the configurations shown in Fig. 106.2 using the fiber from Fig. 106.1 with 250 mW of pump power.

Experimental Results

Under the guidance of **Amplified Spontaneous Emission Considerations** (p. 63), a double-pass polarized amplifier was constructed that contained both the bandpass filter and the

WDM and utilized a Faraday mirror with a polarizing beam splitter (PBS) to separate input from output and preserve the linear polarization state. This amplifier configuration is shown in Fig. 106.5 and utilizes both single-mode (SM) and PM fibers. The input signal comes through a PM-pigtailed isolator to prevent any ASE or signal from returning to the seed source. The light then passes through a PM-pigtailed polarizing beam splitter followed by a single-mode, 1030-nm/1053-nm wavelength division multiplexer (WDM) used to reduce ASE. A SM WDM combines the seed light with pump light from a fiber Bragg grating-stabilized pump laser with a second WDM in series for additional isolation of the pump diode from the amplified signal. The combined light is sent into 3.6 m of single-mode, single-clad, ytterbium-doped fiber with an unsaturated absorption coefficient of approximately 70 dB/m at 975 nm. After the first pass of amplification, the signal passes through a Faraday mirror, a factory-aligned, fiber-coupled package containing a Faraday rotator, 10-nm bandpass filter at 1053 nm, and mirror. The reflected light passes back through the Faraday mirror package, the Yb-doped fiber, and the WDM's, one of which acts to filter out the ASE centered at 1030 nm (WDM1). Since the polarization at the PBS is orthogonal to that which entered the PBS because of the Faraday mirror, the light is ejected out a different port and sent through a PM 90/10 splitter to provide polarized signal and sample ports. All fibers were spliced using a Furukawa S183PM fusion splicer, and there are no alignment knobs in the system. The pump was operated continuously and there is no AOM gate so that no temporal alignment is required between the seed pulses and the amplifier.

The seed pulse used in this amplifier was a 2-ns square pulse with 1.56 pJ of energy, resulting in a peak power of 0.78 mW. The seed pulse had an optical wavelength of 1053 nm and a pulse repetition rate of 300 Hz and was linearly polarized with a polarization extinction ratio of 20 dB. Different lengths of Yb-doped fiber were tested in the amplifier to optimize the active fiber length in terms of maximizing gain while maintaining stability as well as operation free from parasitic lasing or self-pulsations. For a given fiber length, a fraction of the fiber remains unpumped and thus lossy to the signal wavelength. If the pumped portion of the fiber has sufficient gain, then the amplifier can *Q*-switch because of the saturable absorption of the unpumped section of fiber and minute reflections in the system. This can be remedied by making the fiber sufficiently short; however, there is an optimum fiber length for which the fiber provides maximum gain without self-pulsations. For several amplifiers that were constructed, the optimum fiber length



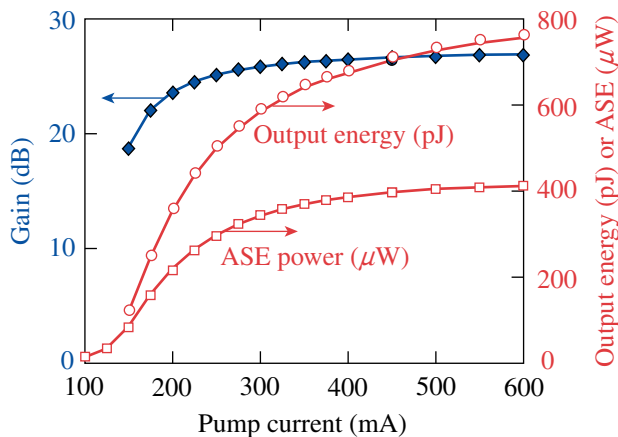
E13545JRC

Figure 106.5

Schematic of a high-gain, double-pass amplifier consisting of input and output isolators, a polarizing beam splitter (PBS), an ASE/signal wavelength division multiplexer (WDM1), two pump/signal wavelength division multiplexers (WDM2), 3.6 m of ytterbium-doped fiber, a Faraday mirror, and a 90/10 splitter. The Faraday mirror was a factory-aligned package containing a lens (L), Faraday rotator (FR), bandpass filter (F), and mirror (M). The polarization-maintaining fiber is notated by dotted lines while the single-mode fiber is notated in solid.

was determined to be near 3.5 m, regardless of the variability between components or splice quality. The pump utilized had a threshold of 16 mA and a slope efficiency of 0.68 mW/mA.

Figure 106.6 shows the signal gain, output energy, and total ASE power as a function of pump current. As the pump current is increased beyond 200 mA, the amplifier gain rolls off since the additional pump light is mostly not absorbed in the active fiber, a feature that is also reflected in the ASE curve. It is important to note that because of the low seed energy and repetition rate, the amplifier is unsaturated. Consequently, the



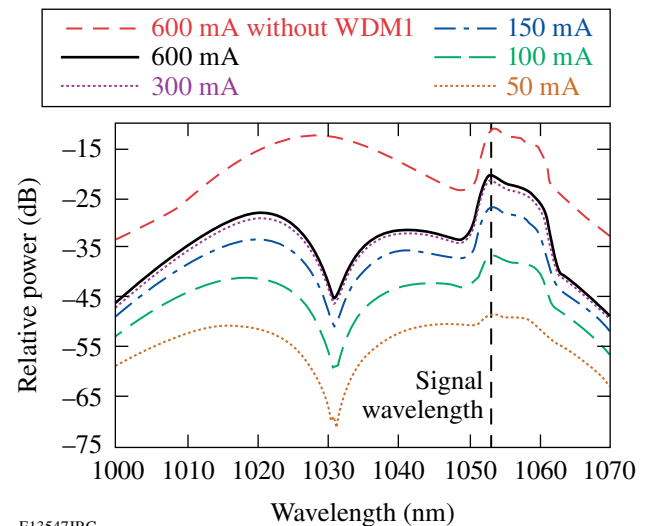
E14258JRC

Figure 106.6

Gain, output energy, and ASE power of the experimental amplifier described in Fig. 106.5 as a function of pump current.

small-signal gain afforded by this amplifier 23 nm off the gain peak is nearly 27 dB.

Self-pulsations were not observed at any pump currents because of the bandpass filter in the Faraday mirror assembly and the 1030-nm/1053-nm WDM that suppresses the stronger gain at shorter wavelengths. Figure 106.7 shows the ASE spectra of the double-pass amplifier for various pump current levels.



E13547JRC

Figure 106.7

Amplified spontaneous emission spectra from a dual-pass fiber amplifier for various pumping levels. Also shown are the seed wavelength at 1053 nm and the ASE trace for the amplifier without the 1030-nm/1053-nm WDM, which has been offset for clarity.

The seed wavelength is depicted by the vertical dashed line. The traces clearly show the double-pass gain of the wavelengths in the filter pass band compared to the single-pass gain of those outside the pass band. The top trace in Fig. 106.7, which is offset for clarity, is the ASE spectra for the double-pass amplifier without the 1030-nm/1053-nm WDM. This WDM, combined with the 10-nm bandpass filter, has a significant impact on both the output of the amplifier and the stability against lasing and self-pulsations, as evident in Fig. 106.7, and shows results very similar to the modeling results shown in Fig. 106.4.

It is difficult to define the noise floor of a system with regards to a low-repetition-rate signal. Simply comparing the strength of the signals on an optical spectrum analyzer requires an optical gate such that the spectrum is only integrated for the duration of the pulse. One alternative method compares the peak power of the amplified signal to the ASE power. A more meaningful metric that more accurately represents an optical signal-to-noise figure of merit compares the peak power of the amplified pulse to the ASE power in a limited spectral bandwidth around the seed-pulse wavelength. While the total noise floor is less than -28 dB across the entire operating range, the bandwidth-limited noise floor is better than -48 dB in a 0.1-nm bandwidth around the signal wavelength. Since the amplifier runs unsaturated, the noise floor is essentially constant as a function of pump current.

As mentioned previously, the combination of a Faraday mirror and polarizing beam splitter allows for high-fidelity separation of the input and output signals at the front end of the amplifier while maintaining the linear polarization state of the seed. The polarization extinction of the amplified signal was measured to be 19.9 dB, which is identical to that of the input signal.

Discussion and Conclusions

The pump is a grating-stabilized diode centered at 975.5 nm. The feedback from the fiber Bragg grating (FBG) maintains stable laser operation even in the presence of optical feedback, which can otherwise destabilize a diode laser.⁸ However, the amplified seed can be a problem in damaging the diode. Starting with a 2-pJ seed signal of 2-ns duration, the amplified signal becomes ~ 1 nJ. By some spurious reflection, a second round-trip through the double-pass amplifier is possible, leading to 0.5 μ J. Even in the presence of a pump/signal WDM, the fraction split off from this energetic pulse (~ 15 dB) leads to a pulse impinging on the face of the pump diode with an energy of 15 nJ and a peak power over 7 W. This can cause catastrophic optical damage on the facet of the laser diode

where the beam size is less than 10^{-7} cm². Two components in our system serve to eliminate this problem. The first is the output isolator, which significantly reduces the risk of a high-energy back-reflection into the amplifier. The second is the second pump/signal WDM, which serves as an ~ 15 -dB isolator of the signal pulse into the diode.

The agreement between measurements and simulations is favorable in the prediction of the noise characteristics of the amplifier, as shown in Table 106.III. In particular, using the ratio of small-signal gain over ASE power leads to an amplifier performance metric of 1161 per milliwatt, which agrees exceedingly well with the measurements. Both the signal gain and the ASE power levels were approximately 6 dB too high in the simulations, even when accounting for realistic component loss. There are several reasonable explanations for the discrepancy. First, there is the uncertainty in the loss due to the components and the splices. Second, the addition of the 10-nm filter in the Faraday mirror assembly may cause additional insertion loss due to slight perturbations in the propagation length and/or angle between the mirror and the fiber within the assembly. Finally, some of the parameters used in the simulations were simply taken from previous work.^{6,7} In particular, the emission and absorption cross sections can play a large role in determining the output performance of the amplifier. By varying the simulated emission cross section at 1053 nm, it is found that the ASE and gain change by 9.5% and 8.1%, respectively, for a 1% change in the emission cross section alone. Given the variability between measurements of ytterbium absorption and emission cross sections,^{7,9} this is likely a strong contributor to the mismatch in absolute values of gain and ASE power.

Table 106.III: Comparison of measured and simulated values for the double-pass fiber amplifier.

Characteristic	Measured Value	Simulation Result
Small-signal gain/ASE	1175/mW	1161/mW
Total noise floor	-28 dB	-30.6 dB
Noise floor in 0.1-nm bandwidth	-48 dB	-43.5 dB
Small-signal gain	26.6 dB	32.3 dB

The unpumped amplifier has a passive loss of approximately 15 dB. The simulations show an unpumped amplifier loss of 13.9 dB. While some of this loss is due to absorption in the

unpumped Yb-doped fiber, almost 9 dB of this loss is insertion loss of the constituent components. Many of these components are free-space optics that are packaged with fiber pigtails at the vendor. All-fiber components would certainly help to increase the gain of the system as well as the noise figure. The noise figure of the amplifier is given by¹⁰

$$NF = \frac{2P_{\text{ASE}}}{h\nu\Delta\nu_{\text{opt}}G}, \quad (3)$$

where P_{ASE} is the ASE power measured on a bandwidth $\Delta\nu_{\text{opt}}$, G is the signal gain, and ν is the optical frequency of the signal. Using measured parameters, the noise figure of the double-pass amplifier in a 0.1-nm bandwidth is 6.6 dB. Considering that the seed is degraded by 2.8 dB because of the insertion loss of the components before the active fiber, this result leads us to conclude that, in spite of operating far from the gain peak in a double-pass configuration, the amplifier is of extremely high quality because of the ASE suppression techniques utilized. Further, our model shows that our double-pass amplifier does not add any penalty to the noise figure, as has been observed in erbium-doped amplifiers used in a simple double-pass configuration.⁴

In conclusion, amplified spontaneous emission suppression techniques were utilized to fabricate a double-pass, ytterbium-doped amplifier with the noise properties of a single-pass amplifier. Simulations based on a rate-equation model were used to analyze the ASE and the impact of the suppression techniques. These techniques were implemented in an align-

ment-free, double-pass, ytterbium-doped fiber amplifier with 26-dB gain at a wavelength 23 nm off the gain peak and a -48-dB noise floor while amplifying linearly polarized optical pulses with a low duty cycle.

ACKNOWLEDGMENT

This work was supported by the U.S. Department of Energy Office of Inertial Confinement Fusion under Cooperative Agreement No. DE-FC52-92SF19460, the University of Rochester, and the New York State Energy Research and Development Authority. The support of DOE does not constitute an endorsement by DOE of the views expressed in this article.

REFERENCES

1. E. Desurvire, *Erbium-Doped Fiber Amplifiers: Principles and Applications* (Wiley, New York, 1994).
2. S. Hwang *et al.*, IEEE Photonics Technol. Lett. **13**, 1289 (2001).
3. A. Galvanauskas *et al.*, Opt. Lett. **26**, 935 (2001).
4. S. W. Harun, P. Poopalan, and H. Ahmad, IEEE Photonics Technol. Lett. **14**, 296 (2002).
5. L. L. Yi *et al.*, IEEE Photonics Technol. Lett. **16**, 1005 (2004).
6. Y. Wang and H. Po, J. Lightwave Technol. **21**, 2262 (2003).
7. R. Paschotta *et al.*, IEEE J. Quantum Electron. **33**, 1049 (1997).
8. R. W. Tkach and A. R. Chraplyvy, J. Lightwave Technol. **LT-4**, 1655 (1986).
9. N. A. Brilliant *et al.*, J. Opt. Soc. Am. B **19**, 981 (2002).
10. P. C. Becker, N. A. Olsson, and J. R. Simpson, *Erbium-Doped Fiber Amplifiers: Fundamentals and Technology* (Academic Press, San Diego, 1999).